Supplementary Information

Enhanced environmental adaptability of sandwich-like MoS_2/Ag/WC nanomultilayer film via Ag nanoparticle diffusion-dominated defect repair

Min Yang,[a,b] Xin Fan,[a,b] Siming Ren,[*a] and Liping Wang[*a]

[a.] *Key Laboratory of Advanced Marine Materials, Ningbo Institute of Materials Technology and Engineering, Chinese Academy of Sciences, Ningbo 315201, China.*

[b.] *University of Chinese Academy of Sciences, Beijing 100049, China.*

*Corresponding Authors:

Email: rensiming@nimte.ac.cn (Siming Ren); wangliping@nimte.ac.cn (Liping Wang)

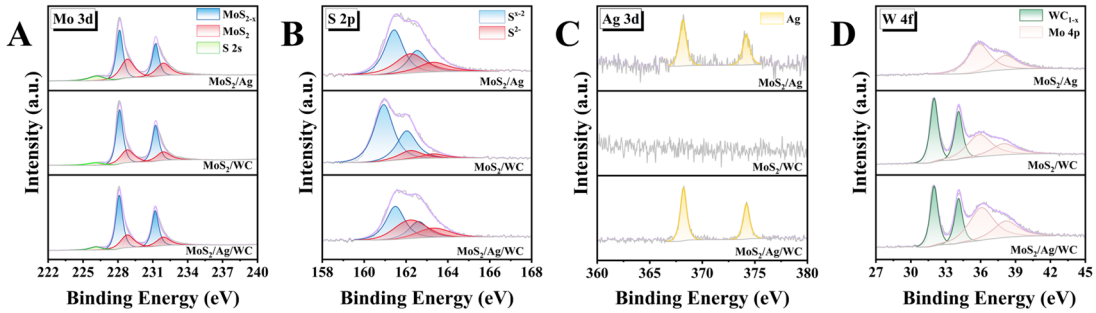

Fig. S1 Chemical bonding analysis of sandwich-like MoS_2/Ag/WC nanomultilayer film and reference films. (A) Mo 3d. (B) S 2p. (C) Ag 3d. (D) W 4f.

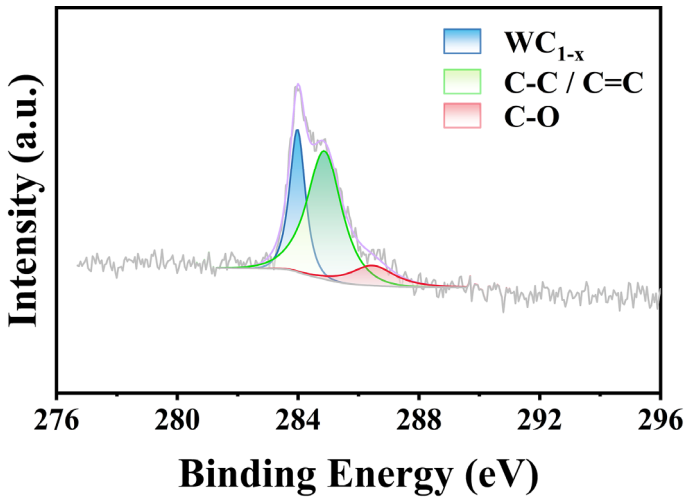

Fig. S2 XPS C 1s spectrum of sandwich-like MoS_2/Ag/WC nanomultilayer film.

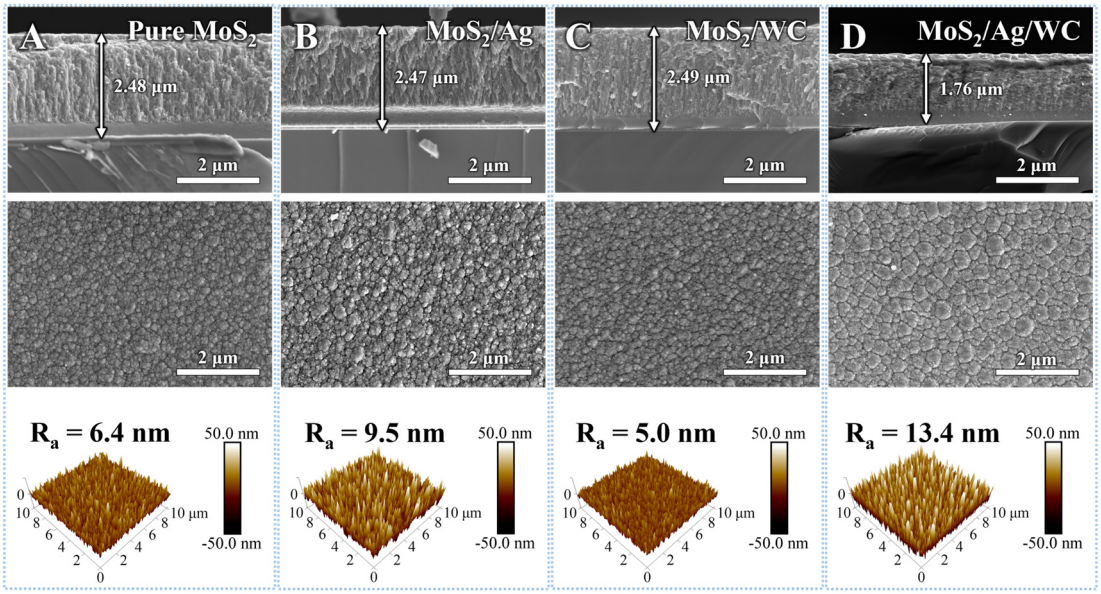

Fig. S3 Morphologies and structures of sandwich-like MoS_2/Ag/WC nanomultilayer film and reference films. (A-D) Cross-section, surface SEM images and SPM images illustrating structures and topographic variations of sandwich-like MoS_2/Ag/WC nanomultilayer film and reference films.

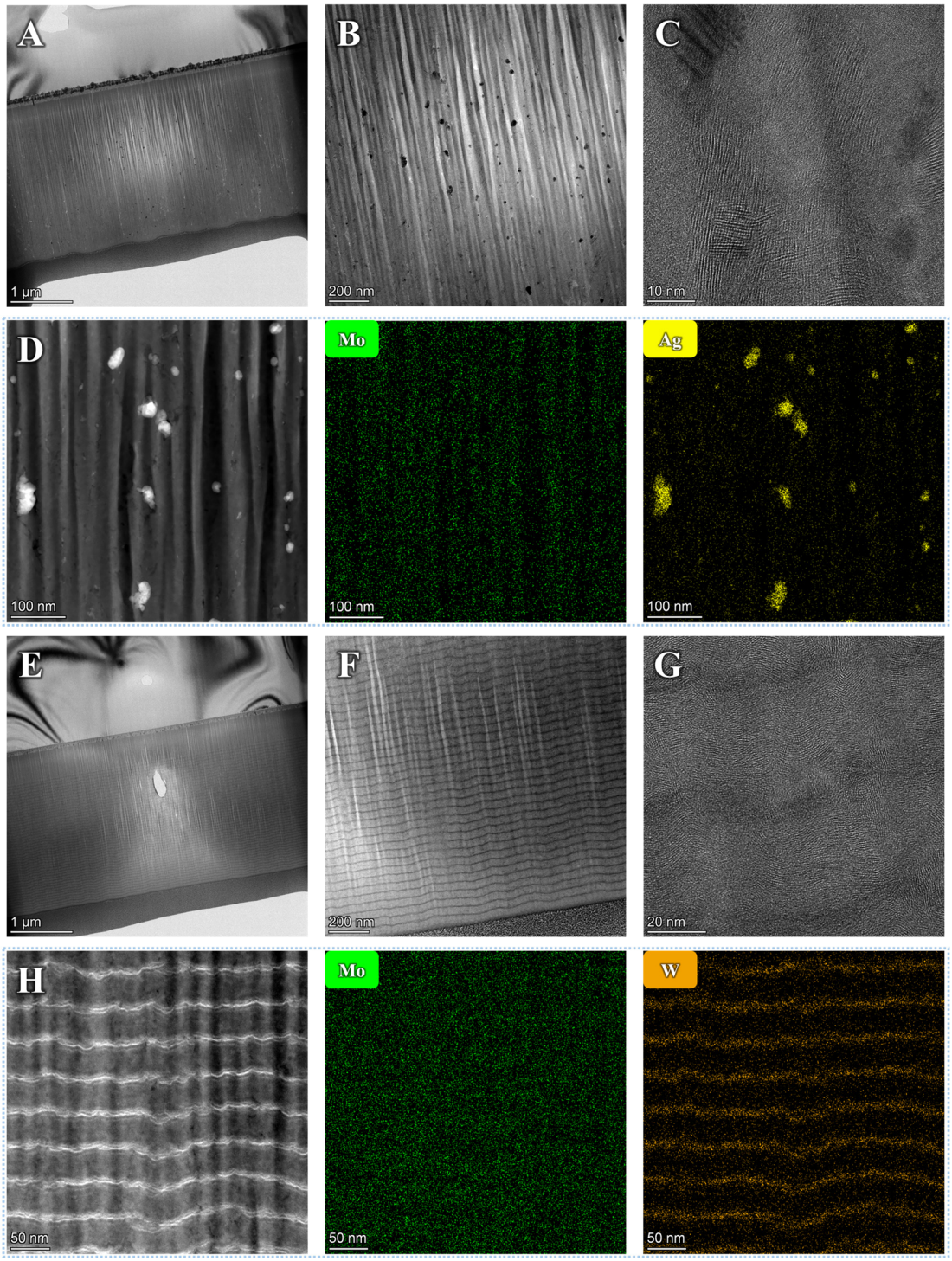

Fig. S4 Structural characterization and interface analysis of MoS_2/Ag composite film and MoS_2/WC nanomultilayer film. (A-B) Low and high magnification TEM images showing cross-sectional view of MoS_2/Ag composite film, respectively. (C) Detailed HRTEM image exhibits the randomly oriented MoS_2(002) planes and Ag NPs. (D) STEM-HAADF micrograph and corresponding EDS maps (Mo, Ag) of MoS_2/Ag composite film. (E-F) Low and high magnification TEM images showing cross-sectional view of MoS_2/WC nanomultilayer film, respectively. (G) Detailed HRTEM image exhibits the alternating growth of MoS_2(002) layers and amorphous WC layers. (H) STEM-HAADF micrograph and corresponding EDS maps (Mo, W) of MoS_2/WC nanomultilayer film.

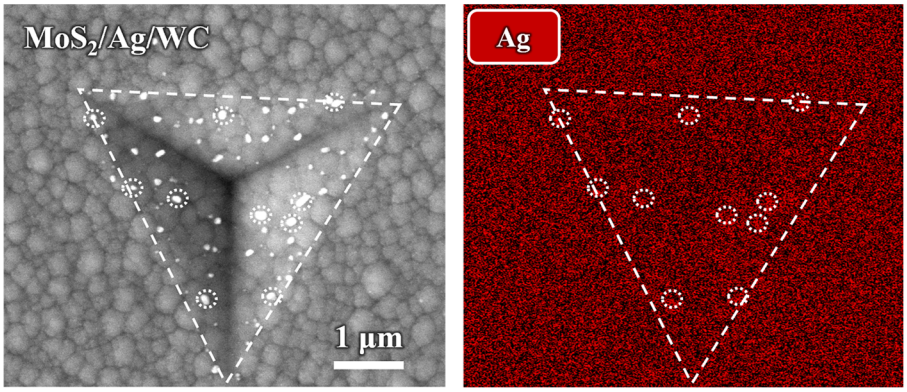

Fig. S5 Indentation morphology of sandwich-like MoS_2/Ag/WC nanomultilayer film and corresponding EDS map demonstrating an Ag enrichment in particles marked by white dash circles.

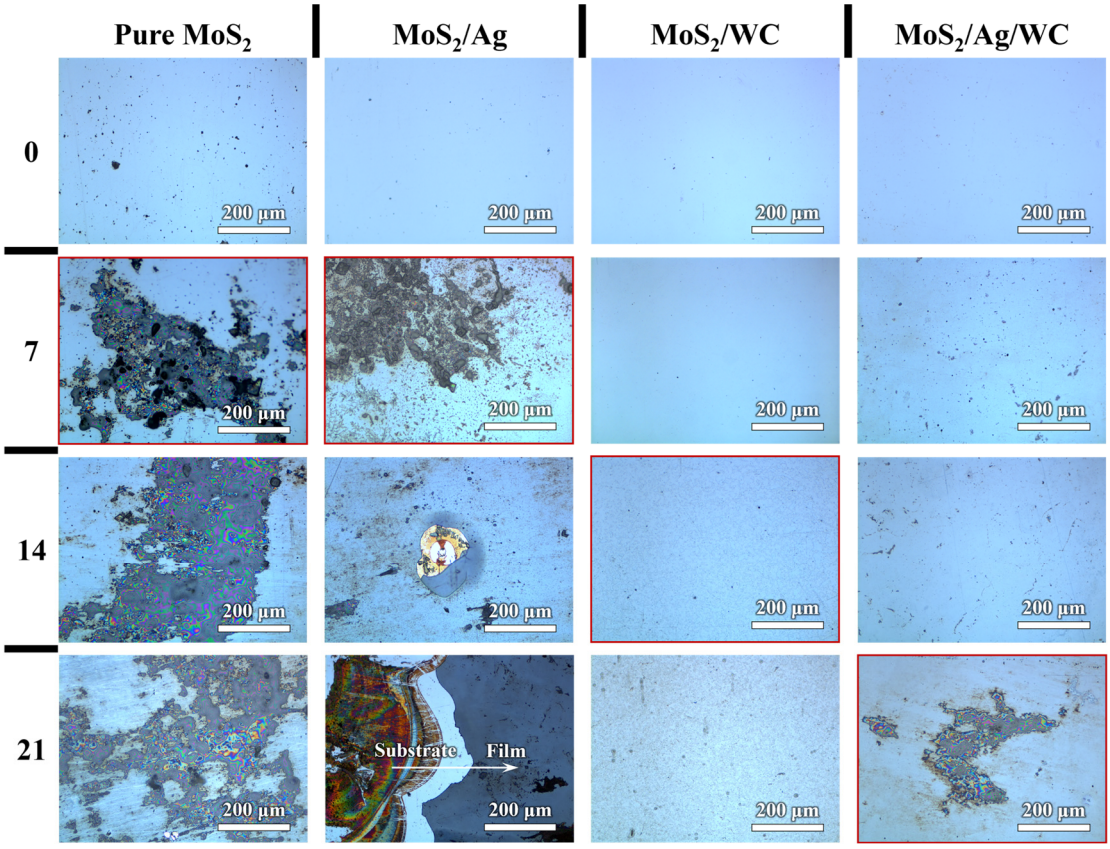

Fig. S6 Optical surface morphologies of sandwich-like MoS_2/Ag/WC nanomultilayer film and reference films during the 21-day salt spray process.

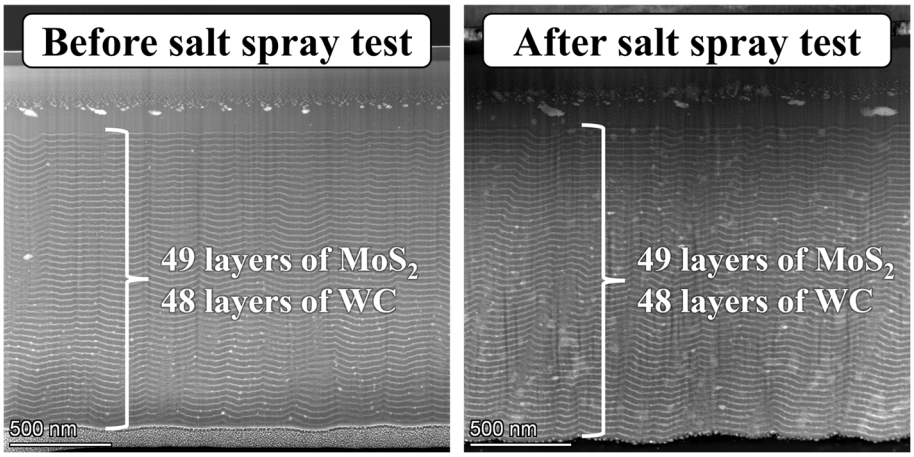

Fig. S7 Modulation period counting of sandwich-like MoS_2/Ag/WC nanomultilayer film before and after salt spray tests of 21 days.

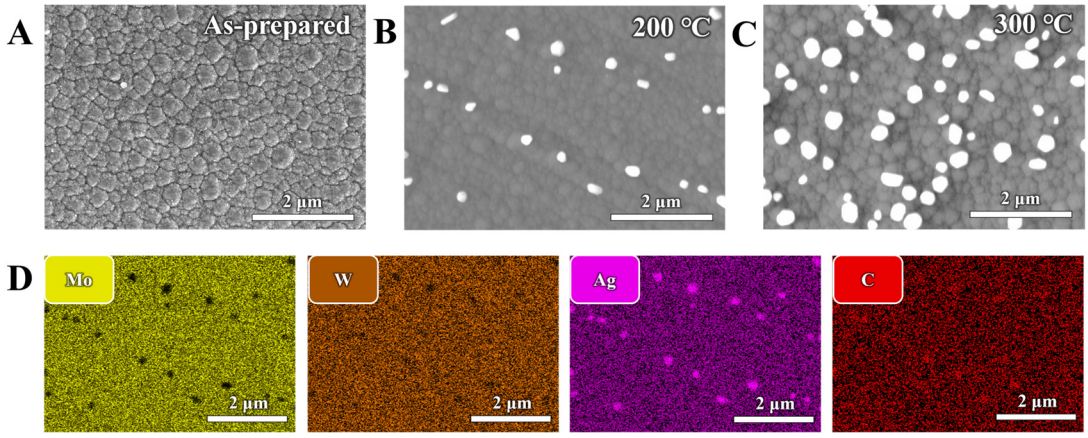

Fig. S8 Ag diffusion behavior under vacuum annealing of elevated temperatures. (A-C) SEM images of as-prepared (A), 200 °C (B) and 300 °C (C) vacuum annealing surface of the sandwich-like MoS_2/Ag/WC nanomultilayer films. (D) Corresponding EDS maps (Mo, W, Ag, C) of (B).

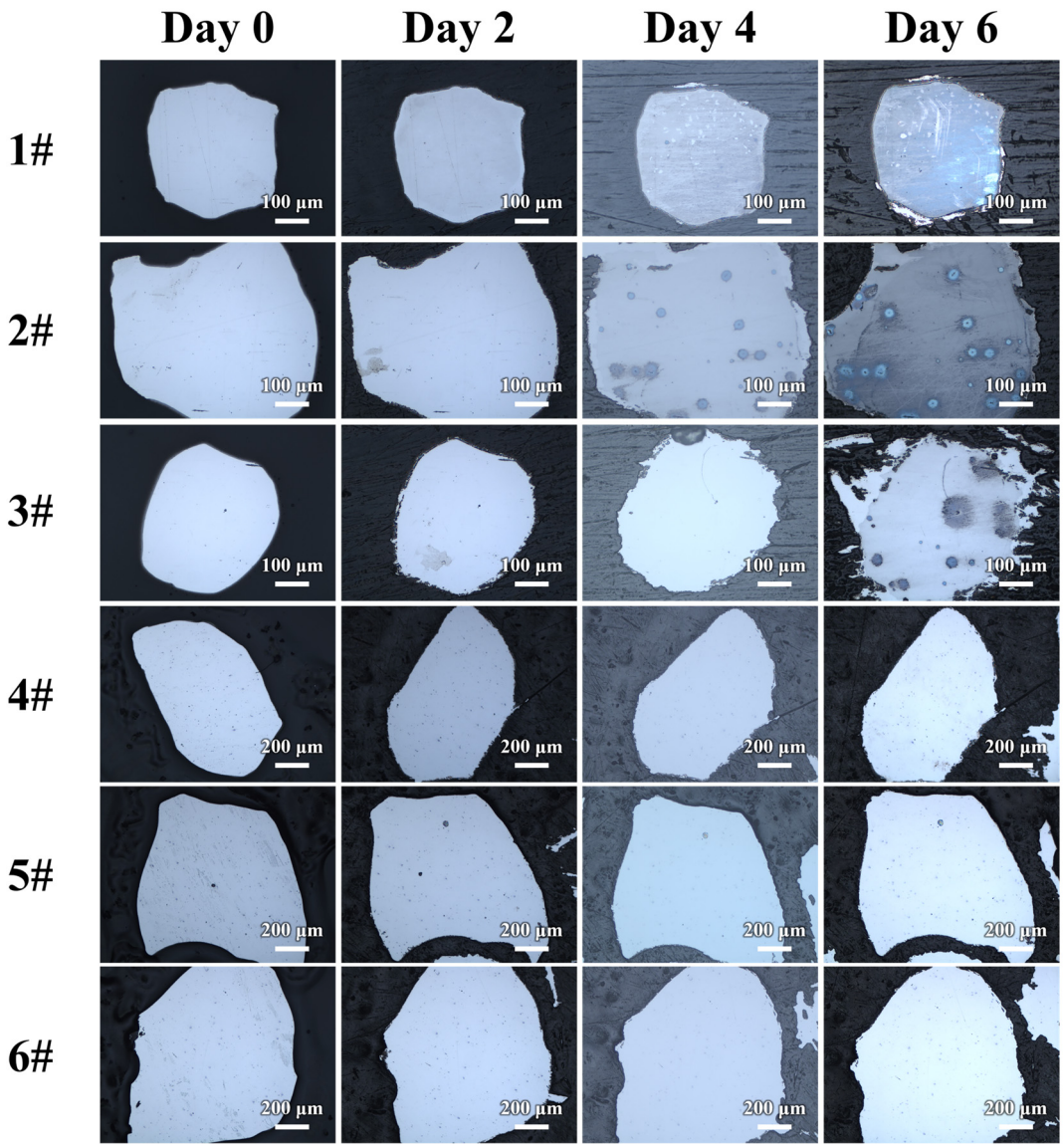

Fig. S9 Optical images of the sandwich-like MoS_2/Ag/WC nanomultilayer films for as-prepared state (1#~3#) and 36 months air exposure (4#~6#) after 0, 2, 4, 6 days of salt spray.

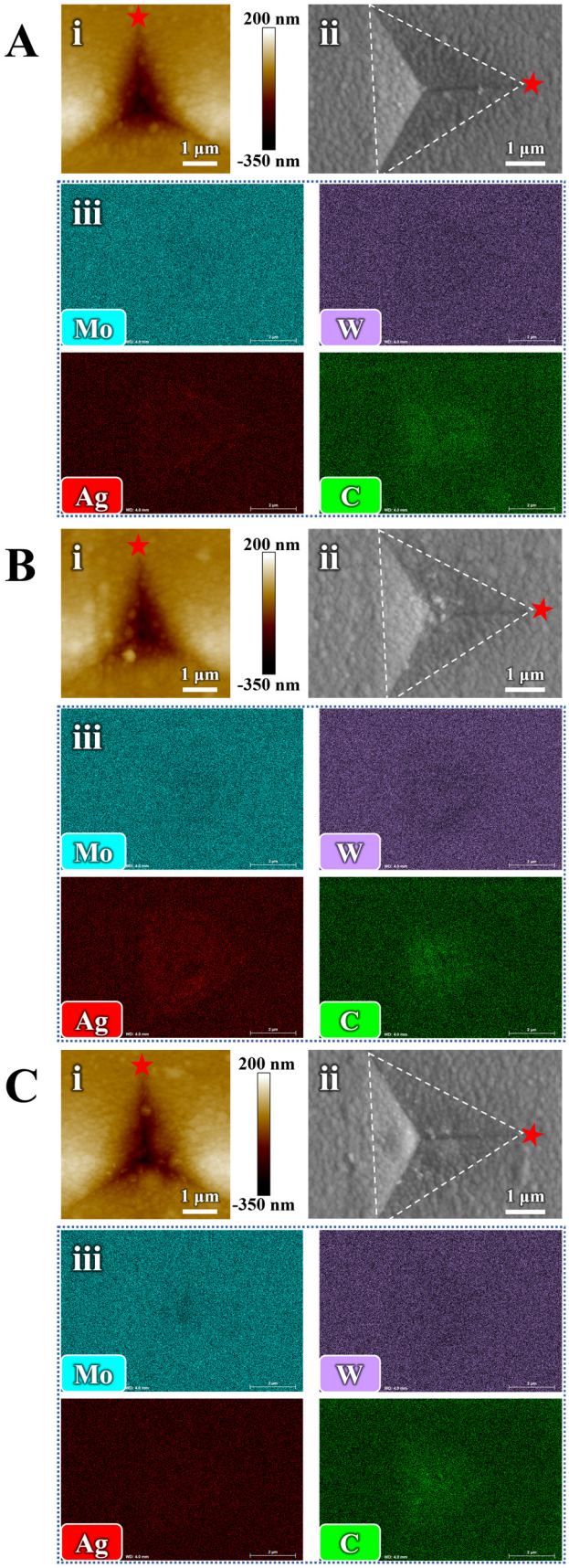

Fig. S10 Diffusion behavior of three random nanoindentations for the sandwich-like MoS_2/Ag/WC nanomultilayer films. (A-C) Topographical images (i), surface potential distributions (ii), SEM images (iii) and corresponding EDS Mo, W, Ag and C maps (iv) on nanoindentations after 6 days of salt spray, the five-pointed star indicates the identical position of each indentation.

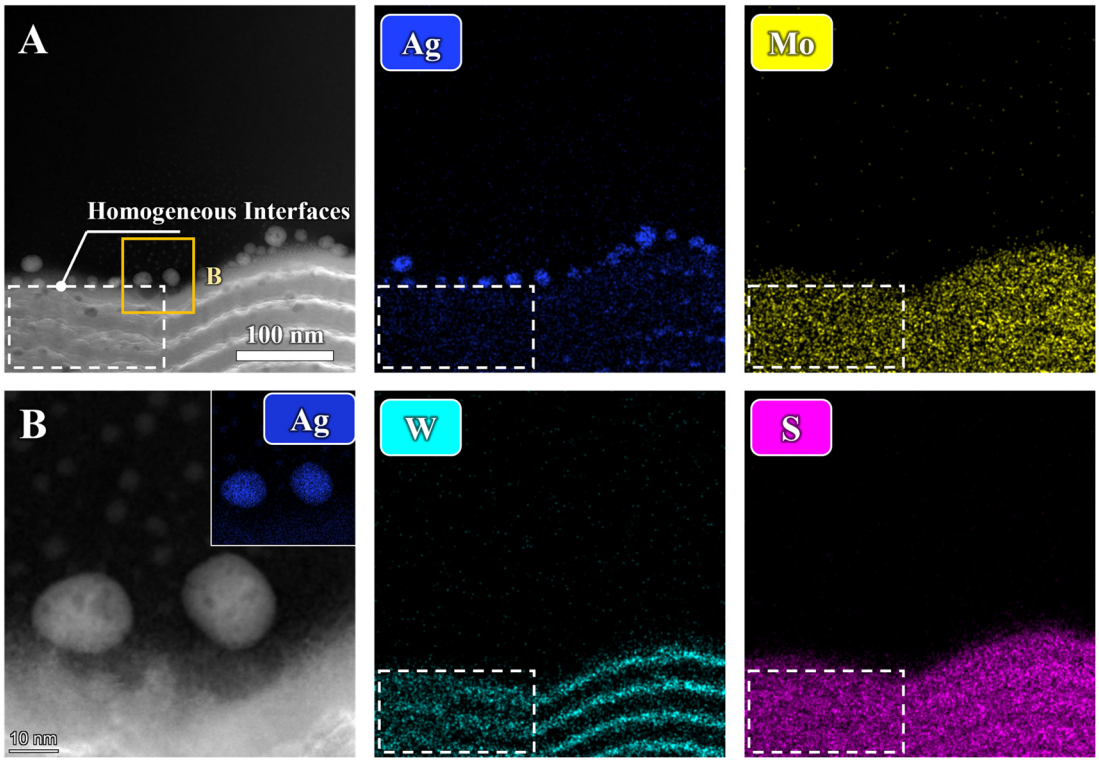

Fig. S11 Cross-sectional composition and morphology of the sandwich-like MoS_2/Ag/WC nanomultilayer film after 21days of salt spray plus 18 months of air exposure. (A) The STEM-HAADF image and corresponding EDS maps (Mo, W, Ag, S) reveal a mixed interface marked by white dash frame after long-term corrosion test. (B) Enlarged view and corresponding EDS Ag map illustrating the particle size and structure on the top surface.

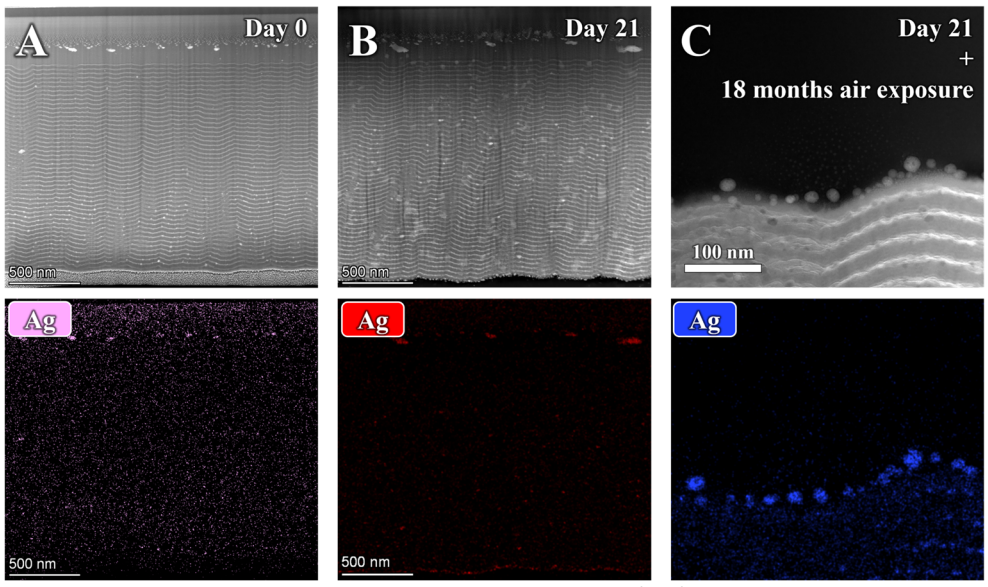

Fig. S12 Ag NPs diffusion behaviors of the sandwich-like MoS_2/Ag/WC nanomultilayer films over time. Cross-sectional TEM micrographs and corresponding EDS Ag maps of the sandwich-like MoS_2/Ag/WC nanomultilayer film before (A) and after (B) 21 days of salt spray, and (C) 18 months air exposure after 21 days salt spray.

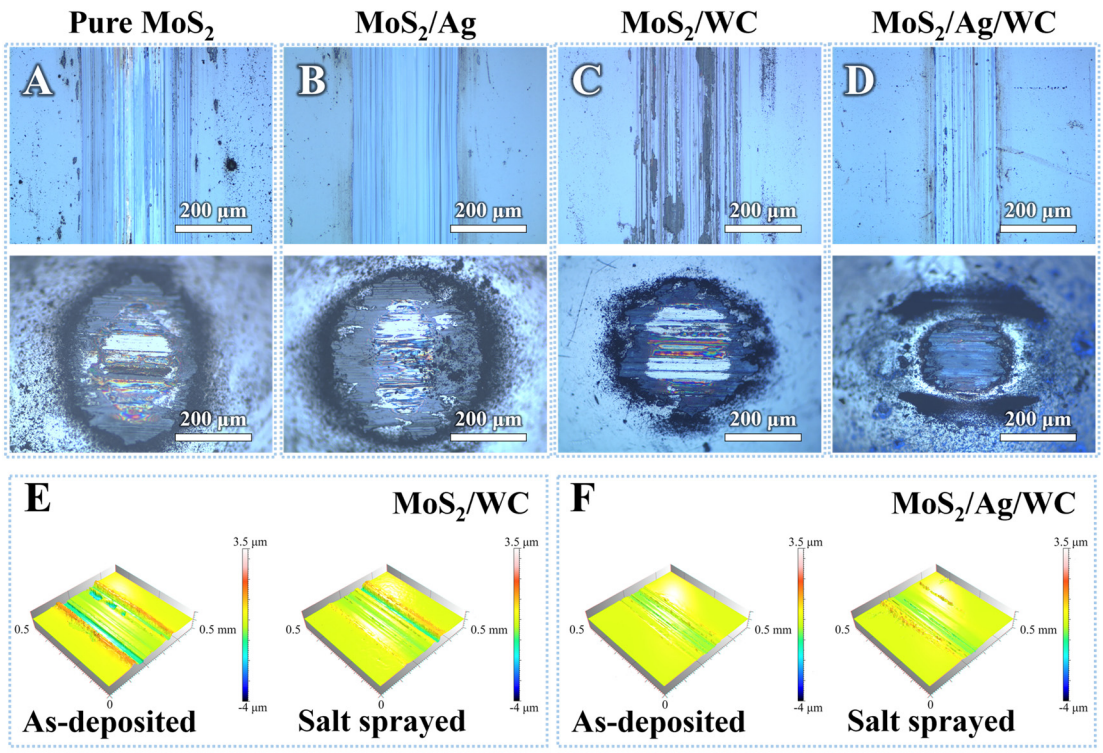

Fig. S13 Characterizations of rubbing surface for the sandwich-like MoS_2/Ag/WC nanomultilayer film and reference films before salt spray tests. (A-D) Optical images on film wear tracks and ball wear scars. (E-F) 3D morphologies of film wear tracks obtained from MoS_2/WC and MoS_2/Ag/WC nanomultilayer films before and after salt spray tests of 21 days.

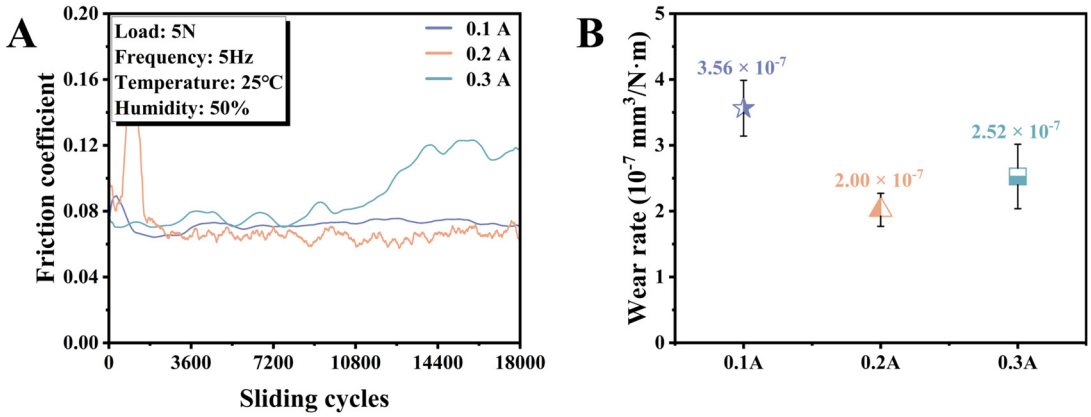

Fig. S14 Tribological performance of the sandwich-like MoS_2/Ag/WC nanomultilayer films with varying Ag target currents. Friction curves (A) and wear rates (B) of the sandwich-like MoS_2/Ag/WC nanomultilayer films (Ag target current: 0.1 A, 0.2 A and 0.3 A).

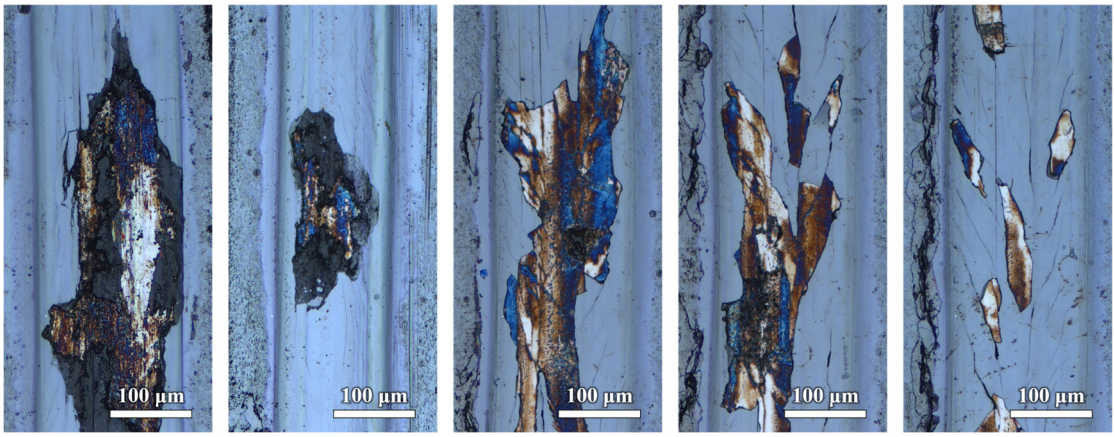

Fig. S15 Optical images on repeated film wear tracks of five different film wear tracks for the MoS_2/WC nanolayered films after salt spray test of 21 days.

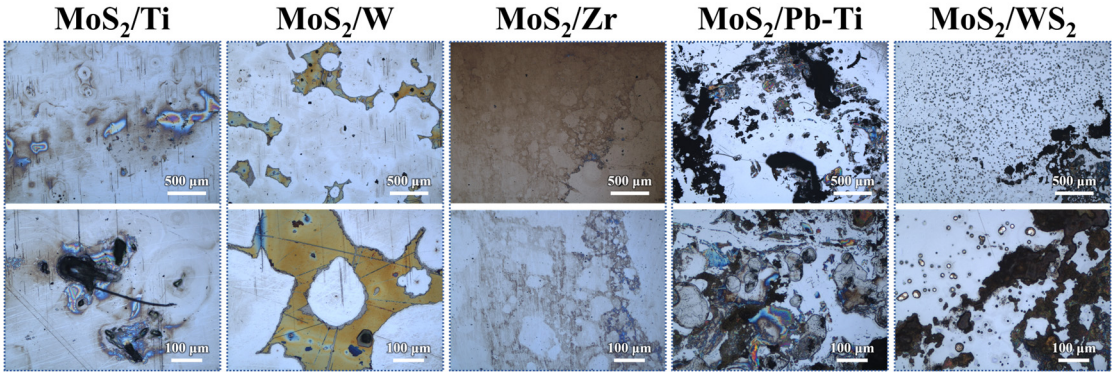

Fig. S16 Optical photographs of MoS_2-based films, including MoS_2/Ti, MoS_2/W, MoS_2/Zr, MoS_2/Pb-Ti, and MoS_2/WS_2, after 14 days of salt spray testing.

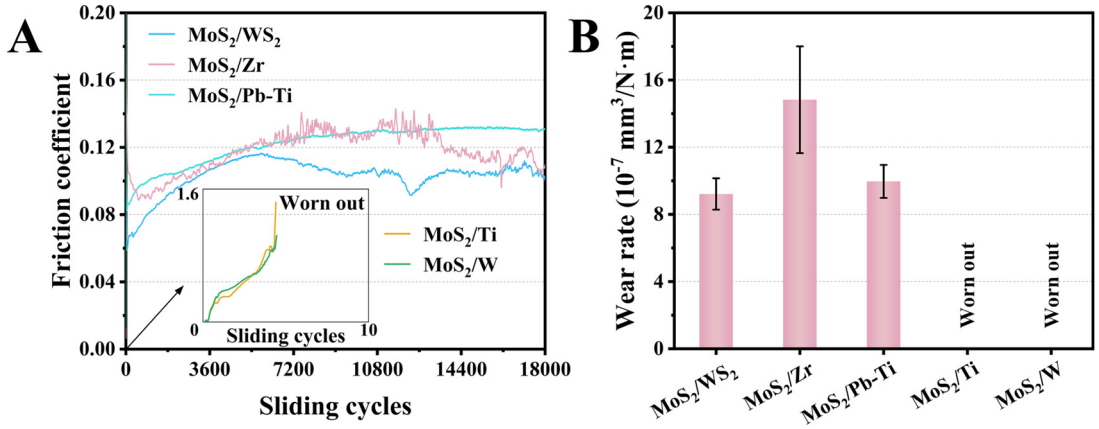

Fig. S17 Friction curves (A) and average wear rates (B) of reported state-of-art MoS_2-based (Ti, W, Zr, Pb-Ti, WS_2) films after 14 days of salt spray.

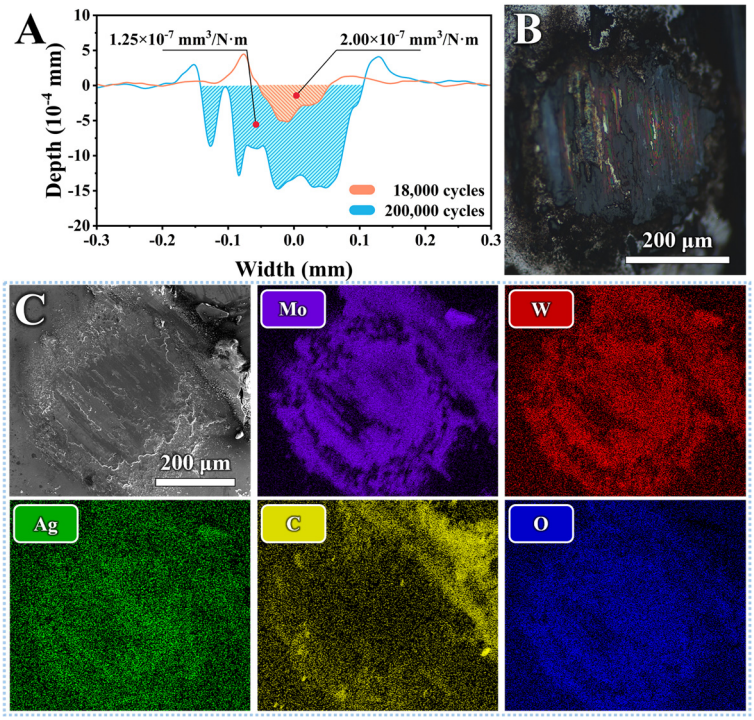

Fig. S18 Wear behavior and characterization of MoS_2/Ag/WC nanomultilayer film after long-term tribological test. (A) Cross-sectional profiles showing wear volume before and after long-term tribological tests, with the corresponding calculated wear rate labelled. (B) Optical image of ball wear scar generated by MoS_2/Ag/WC nanomultilayer film after the long-term tribological test. (C) Corresponding SEM image and EDS maps (Mo, W, Ag, C, O) of the optical image shown in (B).